HHS Public Access

Author manuscript

Brain Struct Funct. Author manuscript; available in PMC 2018 January 01.

Published in final edited form as:

Brain Struct Funct. 2017 January ; 222(1): 131–149. doi:10.1007/s00429-016-1205-1.

Fgf3 and *Fgf16* expression patterns in the developing chick inner ear

Daniel Olaya-Sánchez[1], **Luis Óscar Sánchez-Guardado**[1], **Sho Ohta**[3], **Susan C. Chapman**[3], **Gary C. Schoenwolf**[3], **Luis Puelles**[2], and **Matías Hidalgo-Sánchez**[1,*]

[1]Department of Cell Biology, School of Science, University of Extremadura, Badajoz E06071, Spain

[2]Department of Human Anatomy and Psychobiology, School of Medicine, University of Murcia, Murcia E30100, Spain

[3]University of Utah, Dept. of Neurobiology and Anatomy, 2R066 School of Medicine, 30 N. 1900 E., Salt Lake City, UT 84132-3401, USA

Abstract

The inner ear is a complex sensorial structure with auditory and vestibular functions. The developing otic epithelium gives rise to neurosensory and non-sensory elements of the adult membranous labyrinth. Extrinsic and intrinsic signals manage the patterning and cell specification of the developing otic epithelium by the establishment of lineage-restricted compartments defined in turn by differential expressions of regulatory genes. FGF3 and FGF16 are excellent candidates to govern these developmental events. In the chick, we showed that *Fgf3* expression was present in the borders of all developing cristae. Strong *Fgf16* expressions were detected in a portion of the developing vertical and horizontal pouches, whereas the cristae showed weaker or undetected *Fgf16* expressions at different developmental stages. Concerning the rest of the vestibular sensory elements, both the utricular and saccular maculae were *Fgf3* positive. Interestingly, a strong *Fgf16* expression delimited these *Fgf16*-negative sensory patches. The *Fgf3*-negative macula neglecta and *Fgf3*-positive macula lagena were included within weakly *Fgf16*-expressing areas. Therefore, different FGF-mediated mechanisms might regulate the specification of the anterior (utricular and saccular) and posterior (neglecta and lagena) maculae. In the developing cochlear duct, the dynamic *Fgf3* and *Fgf16* expressions suggest their co-operation in the early specification and later cell differentiation in the hearing system. The requirement of *Fgf3* and *Fgf16* genes in endolymphatic apparatus development and neurogenesis are discussed. Based on these observations, FGF3 and FGF16 appear to be key signaling pathways to control the inner ear plan by means of defining epithelial identities within the developing otic epithelium.

Keywords

Fibroblastic growth factors; otic specification; sensory patch; acoustic-vestibular ganglion; otic innervation

[*]Correspondence to: Matías Hidalgo-Sánchez; Department of Cell Biology, University of Extremadura, Avda. de Elvas s/n, 06071 Badajoz, Spain. Tel. and Fax: +34 924289411, mhidalgo@unex.es.

INTRODUCTION

The inner ear is an elaborate three-dimensional sensory organ which mediates hearing and balance functions. This sensory organ arises from the otic placode, a flat and thickened portion of the cephalic ectoderm located on each side of the developing hindbrain. The otic placode derives from a common *Pax2*-positive placode-epibranchial-epidermis field. FGF and the canonical WNT/β-catenin signaling pathways cooperate to regulate the acquisition of the placode-epibranchial fate decisions, assigning specifically the otic identity to the dorsalmost part of that *Pax2*-expressing area (Ohyama et al. 2007; Bok et al. 2007; Hans and Westerfield 2007; Schimmang 2007; Freter et al. 2008; Ladher et al. 2010; McCarroll et al. 2012). In the chick, a fate mapping study at the 10-somite stage, using the chick/quail experimental model, has recently shown that the otic placode is included within the cephalic ectoderm facing rhombomeres (rh) 4, rh5, and RhC (Sánchez-Guardado et al. 2014). Antagonistic local activation/inhibition phenomena could then be directly involved in early differential fates of the otic placode through a flat Cartesian positional model of intercrossing longitudinal and paraneuromeric transverse domains, above all relative to the two main orthogonal body axes, anteroposterior (AP) and dorsoventral (DV) (Sánchez-Guardado et al. 2014). Thus, the avian otic placode is subdivided into three longitudinal bands of specification domains, arranged dorsoventrally: (1) the dorsalmost band will generate the endolymphatic apparatus; (2) the middle band will develop into the maculae plus the macular-derived basilar papilla, as well as their attached non-sensory epithelia; and (3) the ventralmost band will generate the cristae and their associated semicircular canals (Sánchez-Guardado et al. 2014). Knowledge of the accurate topological position of the presumptive domain of each inner ear component within the otic placode is therefore useful to comprehend the early patterning and specification occurring during the development of this intricate sensory organ.

The otic placode invaginates and then pinches off to form a simple sac-like otocyst. This otic vesicle gives rise after that to an apparently complex three-dimensional sensory organ through varied inductive and morphogenetic events, governed by diffusible signaling pathways from the nearby tissues and the otic epithelium itself through multi-step mechanisms (Bok et al. 2007; Ladher et al. 2010; Groves and Fekete 2012; Chen and Streit 2013). Final cell fate specifications, differential growth, and morphogenesis in the developing membranous labyrinth could occur through asymmetric transcription factor expression patterns, which provide positional identities according to a compartmental model (Fekete 1996; Brigande et al. 2000; Fekete and Wu 2002). A complex network of morphogenes, such as FGF, RA, WNT, and BMP, determine directly the regionalization of the developing membranous labyrinth (for the chick inner ear, see: Oh et al. 1996; Wu and Oh 1996; Sánchez-Calderón et al. 2004, 2007a; Stevens et al. 2003; Sienknecht and Fekete 2008, 2009; Sánchez-Guardado et al. 2009; 2013). Despite the interest existing about the molecular and cellular mechanisms involved in inner ear patterning and fate specification of the growing membranous labyrinth, a high number of questions remain to be resolved.

Fibroblast growth factors (FGFs) consist of a structurally linked family of 23 members, grouped into seven subgroups according to their sequences and functional (relative mitogenic) properties (reviewed by Imamura 2014; see also Itoh and Ornitz 2004; Zhang et

al. 2006). It is well known that FGF signaling pathways play a key role in the transition from the otic placode to the otic vesicle, as well as in the early patterning of the otic anlagen (reviewed by Chatterjee et al. 2010; Frenz et al. 2010; Ladher et al. 2010; Groves and Fekete 2012; Chen and Streit 2013). Once the otic vesicle is formed, FGF signaling pathways could determine the early patterning, the specification of sensory *versus* non-sensory elements, and neurogenesis in the developing otic anlagen. The chick *Fgf10* expression is present in a narrow ventromedial band of the otic anlagen at the otocyst stage. This *Fgf10*-expressing area splits repetitively into several separate subdomains when development proceeds, creating six of the eight sensory organs present in birds. Only the lateral crista and the macula neglecta are initially *Fgf10* negative, activating the *Fgf10* expression within them once their specifications take place (Sánchez-Guardado et al. 2013). Additional FGF signaling pathways could also control the arrangement of all these sensory elements in this intricate three-dimensional sensory structure. At the otic vesicle stage, the *Fgf8* expression defines a continuous rostrocaudal band located within the *Fgf10*-expressing domain, contiguous to the *Gbx2* domain, and overlapping the *Otx2* domain at caudal levels (Hidalgo-Sánchez et al. 2000; Sánchez-Guardado et al. 2013). This *Fgf8*-positive patch observed in the otocyst wall could participate in the specification of the macula sacculi and macula lagena, as well as in the medial part of the macula utriculi (Sánchez-Calderón et al. 2002, 2004). Also, *Fgf19* expression is present in the developing macula utriculi and macula lagena, as well as in the borders of various developing sensory elements (Sánchez-Calderón et al. 2007a; Sánchez-Guardado et al. 2013). Therefore, an intricate network of FGF diffusible signals could determine the timetable of sensory specification in the developing otic epithelium.

FGF3 is a good candidate to govern the induction and early patterning of the otic anlagen from the otic placode to otocyst stages (reviewed in Torres and Giraldez 1998; Cantos et al. 2000; Fekete and Wu 2002; Pickles and Chir 2002; Noramly et al. 2002; Fritzsch et al. 2006; Sánchez-Calderón et al. 2007b; Schimmang 2007; Whitfield and Hammond 2007; Chatterjee et al. 2010; Frenz et al. 2010; Ladher et al. 2010; Groves and Fekete 2012; Chen and Streit 2013). As development proceeds, mouse *Fgf3* is reported to be expressed exclusively in the sensory epithelium of vestibular and cochlea organs (Wilkinson et al. 1989; Pirvola et al. 2000), both in sensory hair and underlying supporting cells (Wilkinson et al. 1989). Several *Fgf3* knockout mice show a dysmorphogenesis of the inner ear presenting diverse defects in the endolymphatic apparatus structure (Mansour et al. 1993; Mansour 1994; Hatch et al. 2007), dilated semicircular canals (Mansour et al. 1993) or even loss of them (Hatch et al. 2007), a common utricular and saccular cavity (Mansour et al. 1993), an improperly coiled or even dysgenetic cochlea (Mansour et al. 1993; Hatch et al. 2007), and alterations in the acoustic and/or vestibular ganglion formation (Mansour et al. 1993; Hatch et al. 2007). However, an *Fgf3* knockout mouse strain has no apparent inner ear phenotype (Alvarez et al. 2003). These differences in described phenotypes strongly point to different levels of both penetrance and expressivity for these *Fgf3* mutant mice (Mansour et al. 1993; Hatch et al. 2007). The fact that mouse *Fgf3* expression partly overlaps *Fgf10* expression and that both signaling pathways activate FGFR2(IIIb) strongly suggest a potential redundant control of the mammalian inner ear patterning and morphogenesis (Pirvola et al. 2000).

FGF16 gene belongs to an FGF subfamily, consisting of FGF9/16/20, with a greater affinity for FGFR2c/3c (Zhang et al. 2006). In zebrafish embryos, *Fgf16* expression is reported in the otic vesicle (Nomura et al. 2006). In mammals, *Fgf16* expression is detected in the posterior portion of the mouse otic cup and later in the dorsolateral aspect of the posterior otic vesicle, probably regulating cell fate decisions and/or axis formation (Wright et al. 2003; Hatch et al. 2009). As development proceeds, mouse *Fgf16* expression is present in all three cristae and in a portion of the non-sensory semicircular canals, as well as in the cochlear duct (Hatch et al. 2009). However, disrupting *Fgf16* expression does not leads to any structural or functional otic alterations (Hatch et al. 2009). In the chick embryos, *Fgf16* expression is first detected in the developing inner ear, controlling the early patterning of the otic placode and then regulating at least the later specification of the anterior and posterior cristae (Chapman et al. 2006). Therefore, FGF16 is an excellent candidate to control the early patterning and consequent specification of the developing membranous labyrinth.

The precise involvement of both FGF3 and FGF16 signaling pathways in the specification of sensory and non-sensory epithelia and acoustic-vestibular ganglion formation, as well as the inner ear morphogenesis, remains to be elucidated. In the present study, we look at the spatial and temporal expression patterns of the *Fgf3* and *Fgf16* genes in the embryonic chick inner ear by *in situ* hybridization on serial and parallel cryostat sections from the otic vesicle stage. We compare their expression patterns with that of the *Fgf10* gene and 3A10 immunroeactions, useful markers of sensory patches in the developing chick inner ear (Sánchez-Guardado et al. 2013). The spatial and temporal relationship of the *Fgf3*, *Fgf16*, and *Fgf10* expression patterns described in this work undoubtedly suggest their implication in an intricate molecular network leading to the specification of sensory and non-sensory elements in the developing membranous labyrinth. This detailed analysis allows us to better understand the specification of the developing membranous labyrinth, as well as to plan subsequet experiments devoted to comprehending the possible roles of FGF signaling pathways in the patterning and morphogenesis of vertebrate inner ears.

MATERIALS AND METHODS

Tissue processing

Chick embryos were obtained from fertilized White Leghorn chick eggs incubated in a humidified atmosphere at 38°C. All embryos were treated according to the recommendations of the European Union and of the Spanish government for laboratory animals. Embryos ranging between stages HH14 and HH34 (Hamburger and Hamilton 1951), were fixed by immersion, or via intracardiac perfusion, with 4% paraformaldehyde in 0.1M phosphate-buffered saline solution (PBS, pH 7.4), at 4°C overnight. The fixed embryos were rinsed and cryoprotected in 10% sucrose solution in PBS and embedded in the same buffered sucrose solution with added 10% gelatin. The blocks were frozen for 1 min in isopentane cooled to −70°C by dry ice, and then stored at −80°C. Cryostat serial sections 20 μm thick were cut in the transverse and horizontal planes, mounted as parallel sets on SuperFrost slides, and stored at −80°C until use. Twenty embryos were used per stage.

RNA probes and *in situ* hybridization procedure

The chick *Fgf10* probes were the same as used previously (NM_204696.1; Sánchez-Guardado et al. 2013). For the chick *Fgf3* plasmid, we used BamH1 and T3 enzymes to generate the antisense probes (NM_205327; Patxon et al. 2010). For the chick *Fgf16* plasmid, we used Xba1 and Sp6 enzymes to generate the antisense probes (NM_001044650; Chapman et al. 2006). All riboprobes were labeled with digoxigenin-11-UTP (Roche, Mannheim, Germany) according to the manufacturer's instructions. *In situ* hybridization was performed on cryosections following the methods described by Sánchez-Guardado and co-workers (2009, 2013). The sections were post-fixed with 4% paraformaldehyde in PBS for 10 min and then rinsed with PBS for 15 min. The sections were acetylated in a solution containing 234 ml of H_2O-d, 3.2 ml of triethanolamine (Sigma), 420 ml of 36% HCl, and 600 ml of acetic anhydride. After acetylation, the sections were permeabilized in 1% Triton X-100 for 30 min, and then pre-hybridized at room temperature for 2 h in a solution containing 50% formamide, 10% dextran sulfate (Sigma), 5× Denhardt's solution (Sigma), and 250 mg/ml t-RNA (Roche), in salt solution. Hybridization was performed with 200–300 ng/ml of the probe in the same hybridization solution overnight at 72°C. After hybridization, the sections were rinsed with 0.2% SSC at 72°C for 1–2 h, and then twice with a solution containing 100 mM NaCl and 100 mM Tris-HCl (pH 7.5). After treatment with 10% normal goat serum (NGS) in the same solution for 2 h, the sections were incubated overnight with alkaline phosphatase-conjugated anti-digoxigenin Fab fragments (Roche, 1:3500). The sections were rinsed twice with the same buffer, and then incubated in 100 mM NaCl, 50 mM $MgCl_2$, and 100 mM Tris–HCl (pH 9.5). The colouring reaction was developed with NBT and BCIP (Roche). The sections were rinsed with PBS and coverslipped with Mowiol (Calbiochem, Bad Soden, Germany). No signal was obtained with the sense probes.

Immunohistochemistry staining procedure

The immunoreactions were performed following the indications of Sánchez-Guardado and co-workers (2009, 2011, and 2013). Briefly, cryosections were washed in PBS and incubated with a solution containing 0.1 M lysine monohydrochloride, 1% NGS, and 0.25% Triton X-100 in PBS, to reduce the nonspecific background. Sections were incubated with 3A10 (1:40; Developmental Studies Hybridoma Bank [DSHB], University of Iowa, Ames, IA; Catalog # 3A10). The primary antibody was reacted with biotinylated goat anti-mouse secondary antibody (Sigma, 1:100), and then with ExtrAvidin-biotin-horseradish peroxidase complex (Sigma, 1:200). All antibodies were diluted in a solution containing 1% NGS and 0.25% Triton X-100 in PBS. The incubations were performed without coverslips, and were terminated by rinsing three times with PBS and 0.05% Triton X-100 (PBS-T). After the immunoreactions, the sections were rinsed three times with PBS-T and then coverslipped with Mowiol.

Antibody characterization

Antibody information was provided in Sánchez-Calderón and co-workers (2013). The monoclonal antibody 3A10 was obtained by using as immunogen ventral spinal cord/cyclophosphamide treatment/assorted nervous tissue (from chick nervous tissue). It has been used as a marker for differentiating neurons in the developing chick nervous system

(Yamada et al. 1991; Storey et al. 1992; Hill et al. 1995; Perez et al. 1999). In the developing inner ear, the 3A10 antibody is a useful tool to label axons of the acoustic-vestibular ganglion (AVG) neurons and to aid in the identification of presumptive sensory epithelia (Adam et al. 1998; Sánchez-Calderón et al. 2004, 2005, 2007b; Battisti and Fekete 2008; Sánchez-Guardado et al. 2009, 2011, 2013; see also Sienknecht and Fekete 2008, 2009).

Imaging

All preparations were photographed with a Zeiss Axiophot microscope equipped with a Zeiss AxioCam camera (Carl Zeiss, Oberkochen, Germany) and AxioVision 2.0.5.3. software, and the images were saved in 4-MB TIFF format. These were size-adjusted, cropped, contrast-enhanced, and annotated with Adobe Photoshop version 7.0 software (Adobe Systems, San Jose, CA). All illustrations were produced with Adobe Photoshop software.

RESULTS

Fgf3 and *Fgf16* expression patterns at the otic vesicle stage (HH20)

In chick embryos, it has been reported that *Fgf3* expression is absent in the otic placode and cup (Karabagli et al. 2002; Aragon and Pujades 2009; Abello et al. 2010; Paxton et al. 2010). Therefore, we first studied the *Fgf3* expression pattern at the otic vesicle stage. In transverse sections through the rostralmost portion of the otocyst, a strong *Fgf3* expression was detected in a small area of the ventrolateral wall (long arrow in Fig 1a). Scattered cells with weaker *Fgf3* expression were also detected in the ventromedial wall (short arrow in Fig 1a). In a more caudal section, *Fgf3*-labeling cells were exclusively observed in the ventromedial portion of the otocyst (short arrow in Fig 1d). In both transverse sections, the *Fgf3*-positive domains were always included within an *Fgf10*-expressing sensory domain (between arrowheads in Fig 1a, c, d, f; Sánchez-Guardado et al. 2013). The incipient acoustic-vestibular ganglion showed a low *Fgf3* expression (AVG; Fig 1a, d). In addition, *Fgf3* transcripts were recognized with no trouble in the hindbrain alar plate (asterisk in Fig 1a), exclusively in the area separating contiguous rhombomeres, but not in the body of any rhombomere (rh6 in Fig 1d; see Aragón et al, 2005).

In the development of the chick inner ear, the *Fgf16* expression has been previously described from stages HH8 to HH20 (Chapman et al. 2006). *Fgf16* mRNA was detected early in an anteroposterior domain located at the dorsalmost aspect of the presumptive otic placode (stage HH8). Strong *Fgf16* expression was described in the dorsal lip of the otic anlagen at an early otic cup stage (stage HH12), extending then ventrally with a weaker expression (stage HH13). By stage HH16, the dynamic *Fgf16* expression begins to be restricted to two separate anterior and posterior areas (Chapman et al. 2006). *In situ* hybridization on serial transverse sections through the anterior and posterior poles of the otocyst (HH20; Fig 1b, e) showed strong *Fgf16* expressions in large portions of the lateral and medial walls of the otic primordium (long arrows in Fig 1b, e). *Fgf16* expression was more evident in the lateral wall than in the medial wall. Low levels of *Fgf16* expression were also observed, mainly in ventral contiguous areas (short arrows in Fig 1b). At a rostral level (Fig 1b, c), the ventral border of the lateral stronger *Fgf16*-expressing domain was

coincident with the lateral border of the *Fgf10*-positive domain (lateral arrowheads in Fig 1b, c), whereas the contiguous ventral weaker *Fgf16*-positive area was included within the *Fgf10*-expressing domain (short arrows in Fig 1b, c). This weaker *Fgf16*-labeling area (short arrow in Fig 1b) was coincident with the *Fgf3*-labeling domain (long arrow in Fig 1a). At a caudal level (Fig 1e, f), the *Fgf16*-stained areas (long arrows in Fig 1e) were, however, clearly separate from the *Fgf10*-positive sensory domain (between arrowheads in Fig 1e, f).

In horizontal sections, analysis of the expression patterns of *Fgf3*, *Fgf10*, and *Fgf16* was clear (Fig 1g, l). *Fgf3* expression was confirmed in the ventral part of the otic vesicle (long arrow in Fig 1j), being absent in its dorsal part (Fig 1g). The *Fgf3*-expressing area showed a sharp lateral border, coinciding with the lateral border of the *Fgf10*-positive domain (rostral arrowheads in Fig 1j, l). Scattered cells showed low *Fgf3* expression in the medial wall of the otic anlagen, more perceptible at the caudal pole (short arrows in Fig 1j). These scattered *Fgf3*-positive cells were always located within the *Fgf10*-expressing domain (between arrowheads in Fig 1l). High levels of *Fgf16* expression were detected at both the rostral and the caudal poles of the otic anlagen (long arrows in Fig 1h, k; Chapman et al. 2006). However, the lateral wall of the otic vesicle showed very low levels of *Fgf16* expression in dorsal sections (asterisk in Fig 1h), but not in ventral sections (asterisk in Fig 1k). Therefore, the rostral and caudal domains of strong *Fgf16* expression were connected by this very weak *Fgf16*-labeled area (asterisk in Fig 1h). In the medial wall of the otic vesicle, a large gap of *Fgf16* expression was detected in both the dorsal and the ventral aspects of the otocyst (Fig 1h, k). It is interesting to note that the presumptive domains of the already differentiated anterior and posterior cristae, *Fgf10* positive (between arrowheads in Fig 1i; Sánchez-Guardado et al. 2013), showed evident, although weaker, *Fgf16* expression (between arrowheads in Fig 1h).

A detailed analysis of ventral sections (Fig 1k, l) showed that the strong *Fgf16* expression (rostral long arrow in Fig 1k) delimited the *Fgf3*- and *Fgf10*-expressing domains observed in the rostral aspect of the otocyst (see rostral arrowheads in Fig 1j–l). Note that a very weak *Fgf16* expression was also identifiable within the anterior *Fgf3* and *Fgf10* expressing domains (large arrowhead in Fig 1j for *Fgf3* and short arrows in Fig 1k, l for *Fgf16* and *Fgf10*). At this level, the caudal *Fgf16*-positive domain (caudal long arrows in Fig 1k) overlapped the *Fgf10*-positive domain (see caudal arrowheads in Fig 1k, l), including the area in which the scattered *Fgf3*-positive cells were detected (short arrows in Fig 1j). In ventral horizontal sections, the developing AVG showed heterogeneous and low levels of *Fgf3* expression (AVG in Fig 1j), but not for the *Fgf16* gene (Fig 1k). Figures 5a and 5b summarize all these results at stage HH20.

Fgf3 and *Fgf16* expression patterns at stage HH24

At stage HH24, the inner ear undergoes significant morphogenetic changes. The presumptive territory of almost all sensory patches are clearly identified on sections treated with probes for *Fgf10* and *Cath1* genes, a sensorial and a hair-cell markers, respectively, as well as with 3A10 immunoreactions for otic axons (Sánchez-Guardado et al. 2013). Horizontal sections through a stage HH24 inner ear enabled us to describe the *Fgf3* and *Fgf16* expression patterns (Fig 2). In the vestibular apparatus, the *Fgf3* expression was

observed in the medial border of the innervated anterior crista (ac; short arrows in Fig 2a and arrowhead in Fig 2a′), but not at the borders of the poorly innervated posterior crista (pc; Fig 2a), both sensory patches being clearly identified by the *Fgf10* expression (between arrowheads in Fig 2c). Horizontal sections across the central part of the vestibule showed that the lateral portion of the macula utriculi was *Fgf3* positive (mu; short arrow in Fig 3d). Interestingly, the presumptive domain of the incipient *Fgf10*-negative lateral crista (Fig 2f), which showed some *Cath1*-positive cells (Fig 2d′), develops contiguous to the strongly *Fgf3*-labeled lateral portion of the macula utriculi (Fig 2d). Therefore, a sharp border of *Fgf3* expression delimited clearly the *Fgf10*-expressing macula utriculi and the presumptive domain of the *Fgf3/Fgf10*-negative lateral crista (see the lateralmost arrowhead in Fig 2d, f). The macula sacculi and the macula neglecta were completely devoid of *Fgf3* transcripts (ms in Fig 2d; mn in Fig 2d).

In the vestibule, areas expressing strongly the *Fgf16* gene (long arrows in Fig 2b) bordered the *Fgf10*-positive anterior and posterior cristae (ac and pc; between arrowheads in Fig 2b, c). Some scattered cells expressing weakly the *Fgf16* gene were detected within the anterior and posterior cristae (ac and pc in Fig 2b; also arrowheads in Fig 2b′). However, the incipient lateral crista and an area contiguous to it were strongly labeled by the *Fgf16* expression (lc and long arrow in Fig 2e for ac). Therefore, it is worth noting that the *Fgf16*-positive lateral crista and the *Fgf3/Fgf10*-positive macula utriculi were clearly delimited by a sharp *Fgf3*/*Fgf16* boundary (lateralmost arrowheads in Fig 2d, e, f). Some embryos treated with *Fgf16* probes showed extremely low, or almost undetectable, levels of *Fgf16* expression in the macula utriculi at this developmental stage (not shown). In the caudalmost aspect of the otic rudiment, the macula neglecta was stained by low levels of *Fgf16* expression (mn in Fig 2e).

In the cochlear duct (cd), the presumptive domain of the basilar papilla is easily recognized by a strong *Fgf10* expression (between arrowheads in Fig 2i, l). Regarding the *Fgf3* expression, the caudal part of the *Fgf10*-positive basilar papilla was *Fgf3* positive (bp; Fig 2g, i, j, l). Concerning the *Fgf16* gene, a rostral *Fgf16*-expressing area (long arrow in Fig 2h) bordered the *Fgf10*-positive basilar papilla in the proximal cochlear duct (see the rostralmost arrowheads in Fig 2h, i). This rostral *Fgf16* expression was absent in the distalmost cochlear duct (Fig 2k). In the caudal pole of the otic anlagen, a dorsoventral band of weak *Fgf16* expression could also be detected (short arrows in Fig 2h, l). The weaker *Fgf16* expression partially overlapped the basilar papilla (short arrow in Fig 2h, k), *Fgf10*/*Fgf3*-positive (Fig 2g, i, j, l).

The acoustic-vestibular ganglion (AVG) showed a weaker expression of the *Fgf3* gene (asterisks in Fig 2d, g), the *Fgf16* expression being completely absent in it (asterisks in Fig 2e, h) at this developmental stage. Figures 5c and 5d summarize all these results at stage HH24.

Fgf3 and *Fgf16* expression patterns at stage HH27

At stage HH27, the morphogenetic progress was more evident and all the sensory epithelia could be easily recognized by *Fgf10* expressions and/or sensory patch innervation. In order to better recognize the possible weak expression of the *Fgf3* and *Fgf16* genes, 3A10

immunoreactions were not performed except when confirmation was required. In horizontal sections through the dorsal aspect of a stage HH27 inner ear, *Fgf3* expression bordered the anterior and posterior cristae (ac and pc; Fig 3a), both sensory patches being *Fgf10* positive (between arrowheads in Fig 3a, c). These sensory patches were bordered by domains expressing the *Fgf16* gene (long arrows in Fig 3b), areas corresponding with the proximal portions of the developing vertical pouch (vp; Fig 3b, c). These two cristae were apparently devoid of *Fgf16* expression (between arrowheads in Fig 3b), although we cannot exclude the presence of very low amount of *Fgf16* transcripts (Fig 3b). At this level, a portion of the developing horizontal pouch can be observed which showed very low *Fgf16* expression (hp; Fig 3b). The macula neglecta was *Fgf16* positive (mn in Fig 3b′).

In more ventral horizontal sections through the central portion of the vestibule (Fig 3d–f), *Fgf3* expression was also clearly detected in the (medial) border of the developing *Fgf10*-positive lateral crista (lc; Fig 3d, f). The developing lateral crista was *Fgf16* negative (between arrowheads in Fig 3e), similar to the other cristae (ac and pc in Fig 3b). Its associated horizontal pouch showed a heterogeneous *Fgf16* expression (hp; long arrow in Fig 3e), in some way similar to the vertical pouch (vp; Fig 3b). Note that the border between the lateral semicircular system and the utricule was clearly defined by a markedly high level of *Fgf16* expression (short arrow in Fig 3e). In relation to the utricule (u; Fig 3d), the macula utriculi showed strong *Fgf3* expression (mu in Fig 3d). The wall of the utricule showed different levels of *Fgf16* expression (u in Fig 3e). The macula utriculi was devoid of *Fgf16* expression (mu; Fig 3e). In the saccule, the macula sacculi displayed a slight *Fgf3* expression in its anterior part (ms in Fig 3d, f), this macula being *Fgf16* negative (ms in Fig 3e, f). The saccular epithelium showed a clear *Fgf16* expression in the area contiguous with the utricle, more evident in its caudal portion (asterisks in Fig 3d–f).

In the proximal cochlear duct (Fig 3g–l), *Fgf3* expression was detected in the rostral portion of the *Fgf10*-expresing basilar papilla (bp in Fig 3g; between arrowheads in Fig 3g, l). In the distalmost cochlear duct, the entire basilar papilla was *Fgf3* positive (bp in Fig 3j, l). The adjacent macula lagena was clearly labeled by the *Fgf3* expression (ml in Fig 3j). Regarding the *Fgf16* gene, the *Fgf16* transcripts were located in the developing macula lagena (ml in Fig 3k) and in a very small portion of the basilar papilla (bp; short arrow in Fig 3h; not considered in Fig 5e). Due the proximity of the basilar papilla and the macula lagena in the distalmost cochlear duct, we performed *in situ* hybridization in a transverse section to confirm the *Fgf3*, *Fgf16*, and *Fgf10* expression patterns, aided also by 3A10 immunoreactions (Fig 3m–o). *Fgf3* expression was detected in the distalmost basilar papilla and in the proximalmost macula lagena (bp and ml in Fig 3m), whereas *Fgf16* transcripts were observed exclusively in the proximalmost macula lagena (ml in Fig 3n), the two sensory elements being identified by different *Fgf10* and innervation patterns (Fig 3o). Figures 5e and 5f summarize all these results at stage HH27.

Fgf3 and *Fgf16* expression patterns at stage HH34

Horizontal sections through a stage 34 inner ear showed that, in the vestibular portion, *Fgf3* expression was present in the borders of all *Fgf10*-positive cristae (ac, pc, and lc; between arrowheads in Fig 4a, c, d, f, g, i). *Fgf16* transcripts were detected in the ampullae

epithelium, encircling each crista (long arrows in Fig 4b, h), and in a small portion of the contiguous semicircular canals (not shown; see Fig 5g, h). Surprisingly, some cells within the cristae domain, adjacent to its borders, expressed weakly the *Fgf16* gene (short arrows in Fig 5b, e; results not considered in the summarizing Fig 5g and h). At this developmental stage, the *Fgf10*-positive macula neglecta can also be clearly observed next, and slightly ventral, to the posterior crista (mn and pc; Fig 4d–f). This vestibular element showed very low levels of *Fgf16* expression (mn in Fig 4e), and was *Fgf3* negative (mn in Fig 4d). In the utricule (u; Fig 4g–i), the macula utriculi showed obvious *Fgf3* expression (mu; Fig 4g). The rest of the utricular wall was *Fgf3* negative (Fig 4g). *Fgf16* expression was detected in the utricular epithelium, particularly in its lateral part, abutting caudally the *Fgf3*-expressing macula utriculi and extending laterally towards the lateral semicircular system (long arrow in Fig 4h). In the saccule, the macula sacculi presented *Fgf3* transcripts in its anterior portion (mu in Fig 4g). Interestingly, this *Fgf3*-expressing area in the saccular macula was contiguous to a dorsoventrally oriented narrow band of low *Fgf16* expression in the anterior saccular wall (short arrow in Fig 4h). The macula sacculi was consequently *Fgf16* negative (Fig 4h).

In horizontal sections across the proximalmost part of the cochlear duct, near the saccule (cd and s; Fig 4g–i), no *Fgf3* expression was appreciated in the cochlear duct (cd; Fig 4g), although a very low level of *Fgf16* expression can be detected in its medial wall (asterisk in Fig 4h). In more ventral sections across the cochlear duct, the basilar papilla can be easily identified (bp; Fig 4j–o). The *Fgf10* expression strongly labels the sensory basilar papilla (pb; between arrowheads in Fig 4l, o) and a contiguous strip of non-sensory epithelium along the neural edge of the basilar papilla (short arrow in Fig 4l; see Sánchez-Guardado et al. 2013). *Fgf3* expression was present in the cochlear duct (Fig 4j, m). Note that *Fgf3* transcripts were detected in the rostral half of the basilar papilla (bp in Fig 4j, l) and in the adjacent non-sensory epithelium (short arrows in Fig 4j, l). *Fgf16* expression was absent at the level of the developing basilar papilla (Fig 4k, n). Regarding the *Fgf10*-positive macula lagena, which develops in the distal cochlear duct (ml; Fig 4m–o), this sensory patch showed a few *Fgf3*-expressing cells on its ventral border (short arrow in Fig 4m). Interestingly, *Fgf16* expression was maintained in this sensory patch, with a stronger expression where the *Fgf3* gene was expressed (short arrow in Fig 4n).

The acoustic ganglion, strongly labeled by the *Fgf10* expression (Fig 4l), showed a reduced group of cells expressing the *Fgf16* gene (short arrow in Fig 4k), but *Fgf3* expressing cells were not detected in this sensory ganglion at this developmental stage (AG in Fig 4j). Figures 5G and 5H summarize all these results at stage HH34.

DISCUSSION

It is now well known that hindbrain-derived FGF3 is directly involved in otic placode induction and specification, in addition to otic anlagen patterning at early developmental stages, following multi-step mechanisms (Torres and Giraldez 1998; Cantos et al. 2000; Fekete and Wu 2002; Maroon et al. 2002; Noramly et al. 2002; Pickles and Chir 2002; Ladher et al. 2005, 2010; Fritzsch et al. 2006; Sánchez-Calderón et al. 2007b; Schimmang 2007; Whitfield and Hammond 2007; Chatterjee et al. 2010; Frenz et al. 2010; Urness et al.

2010; Groves and Fekete 2012; Chen and Streit 2013). Restricted *Fgf3* expression patterns in the adjacent developing hindbrain confirm this statement in several vertebrate species (zebrafish: Phillips et al. 2001, 2003; Kwak et al. 2002; Leger and Brand 2002; Maroon et al. 2002; Maves et al. 2002; Walshe et al. 2002; *Xenopus*: Lombardo et al. 1998; chick: Mahmood et al. 1995; Aragón et al. 2005; Kil et al. 2005; Aragón and Pujades 2009; Abello et al. 2010; mouse: Mahmood et al. 1996; Mckay et al. 1996; Pirvola et al. 2000; Wright and Mansour 2003; Lin et al. 2005; Hatch et al. 2007). FGF3 might also participate in the complex network of intrinsic diffusible signals from the otic placode itself. *Fgf3* expression was reported in this two-dimensional structure in mouse embryos (Mahmood et al. 1996; Mckay et al. 1996; Álvarez et al. 2003; Wright and Mansour 2003; Vazquez-Echevarría et al. 2008; Domínguez-Frutos et al. 2009). However, other works did not detect any *Fgf3* expression in the chick otic placode (Karabagli et al. 2002; Aragon and Pujades 2009; Abello et al. 2010; Paxton et al. 2010), zebrafish (Kwak et al. 2002), or *Xenopus* embryos (Lombardo et al. 1998). We cannot rule out, therefore, the existence of different molecular mechanisms governing the early patterning of the otic placodes of mammalian and non-mammalian vertebrates.

In the otic vesicle, the *Fgf3* expression reported in its ventromedial portion has, however, a pattern common to all vertebrates analysed (zebrafish: Walshe and Mason 2003; Millimaki et al. 2007; Hammond and Whitfield 2011; Sweet et al. 2011; *Xenopus*: Lombardo et al. 1998; mouse: Wilkinson et al. 1989; McKay et al. 1996; Pirvola et al. 2000; Riccomagno et al. 2002; Ozaki et al. 2004; Zheng et al. 2003; Powles et al. 2004; Raft et al. 2004; Arnold et al. 2006; Lillevali et al. 2006; Hatch et al. 2007; Frenz et al. 2010; and chick: this work). The *Fgf3* and *Fgf10* co-expression in the anterior part of the otic vesicle strongly suggests a redundant function of the two signaling pathways, FGF3 and FGF10, in the otic epithelium patterning (Pirvola et al. 2000; Zheng et al. 2003; this work), probably down-regulated by retinoic acid (Frenz et al. 2010). This *Fgf3* expression is also coincident with the neurogenic *Lfng*-expressing domain in the anterior aspect of the otocyst (Riccomagno et al. 2002; Ozaki et al. 2004; Lin et al. 2005; Hatch et al. 2007), whereas *Tbx1* expression is observed in its posterior portion, the later being complementary to the *NeuroD*/*Lfng*/*Fgf3* expressing domain (Raft et al. 2004; see also Abelló et al. 2007). All these findings strongly confirm the involvement of FGF3 in otic sensory specification and neurogenesis at least at the otocyst stage. Due to the existence of scattered *Fgf3*-positive cells in the posterior-medial wall of the otic vesicle, we cannot exclude, however, an additional implication of FGF3 in otic specification (this work).

Mouse *Fgf16* is weakly expressed in the entire otic placode, in the posterior pole of the invaginating otic cup, and in the posterolateral wall of the otic vesicle, suggesting a possible role in otic cell fate decisions as well (Wright et al. 2003; Hatch et al. 2009). In birds, its expression is first detected in the chick otic placode (stage HH8/9), forming an anterior-to-posterior strip just in its dorsalmost aspect (Chapman et al. 2006). *Fgf16* expression is then restricted to the dorsomedial lip of the developing otic cup (HH12) with a weaker expressing domain extending ventrally (HH13; Chapman et al. 2006). At the otic vesicle stage, its dynamic expression leads to a stronger expression at both anterior and posterior poles of the otocyst (Chapman et al. 2006; this work), showing a similar expression pattern to those of the *Bmp4* and PDGF genes (Wu and Oh 1996; Chapman et al. 2006). Therefore, *Fgf16* is

also a strong candidate to govern specifically the early patterning of the otic anlagen in different groups of vertebrates, probably following dissimilar molecular mechanisms.

Specification of the endolymphatic apparatus

The endolymphatic system, a non-sensory element involved in the fluid homeostasis of the inner ear, develops from a dorsally projecting appendage located in the dorsomedial part of the otic vesicle (Sánchez-Guardado et al. 2009). It is widely accepted that FGF3 is directly implicated in the endolymphatic apparatus specification. Although *Fgf3* knockout mice show an apparent normal development of the otic vesicle, these mutants do present a dysmorphogenesis or loss of the endolymphatic apparatus (Mansour et al. 1993; Mansour 1994; Hatch et al. 2007). This phenotype is similar to that observed after FGFR2b(IIIb) disruption, the receptor for FGF3 (Pirvola et al. 2000). $Fgf3^{-/-}/Fgf10^{/+}$ mutant embryos display also an absence of the endolymphatic duct (Zelarayan et al. 2007). Because *Fgf3* expression has not been reported in the developing endolymphatic system in mice at later developmental stages (Wilkinson et al. 1989; McKay et al. 1996; Pirvola et al. 2000), FGF3 from the adjacent developing hindbrain at the otic placode and cup stages would seem to be directly involved in the early specification of the endolymphatic apparatus (Mansour et al. 1993; Mckay et al. 1996; Hatch et al. 2007; Vázquez-Echevarría et al. 2008; see also Wright and Mansour 2003; Domínguez-Frutos et al. 2009; Abello et al. 2010). The distension of the endolymphatic duct following the ectopic expression of *Fgf3* in the chick hindbrain fits well with this assumption (Vendrell et al. 2000). In addition, the lack of the endolymphatic duct in several hindbrain mutants such as $Hoxa1^{-/-}$ (Lufkin et al. 1991), *Kreisler* (McKay et al. 1996; Choo et al. 2006) and in *dreher* (Koo et al. 2009) mutants are consistent with this statement as well. It is also interesting to note that $Wnt1^{-/-}/Wnt8a^{-/-}$ mutant mice show a reduced endolymphatic apparatus, suggesting also a requirement of the WNT signaling pathway for the dorsal patterning of the otic anlagen (Vendrell et al. 2013; see also Riccomagno et al. 2005 and discussion in Sánchez-Guardado et al. 2014).

In birds, the endolymphatic apparatus arises from one of the anteroposterior orientated bands into which the chick otic placode is subdivided. In particular, its presumptive domain corresponds to the dorsalmost stripe, just adjoining the neighbouring developing neural tube and far from the pharyngeal endoderm (Sánchez-Guardado et al. 2014). Interestingly, the *Fgf16*-expressing stripe observed in the chick otic placode (stage HH8/9), anterior-to-posteriorly oriented (Chapman et al. 2006), could correspond to that presumptive domain from which the endolymphatic apparatus arises (Sánchez-Guadado et al. 2014). In addition, the restriction of *Fgf16* expression in the dorsomedial lip of the otic cup (Chapman et al. 2006; HH12–13) suggests a possible involvement of *Fgf16* in the specification of this non-sensory component of the avian inner ear.

Specification of the maculae

The complex network of FGF diffusible signals could also determine the specification of maculae, sensory patches of the membranous labyrinth devoted to linear motion detection. In the chick, the *Fgf10*-expressing sensorial area present in the ventral wall of the otocyst splits repetitively into several disconnected subdomains as development proceeds, creating six of the eight sensory organs present in birds. Only the presumptive domain of the macula

neglecta and the lateral crista start from being *Fgf10* negative to become *Fgf10* positive after their specification as sensory elements (Sánchez-Guardado et al. 2013). Also, *Fgf8* could participate in the arrangement of the macula sacculi and macula lagena, as well as in the specification of the medial part of the macula utriculi (Sánchez-Calderón et al. 2002, 2004). Besides, *Fgf19* expression could regulate the development of both the macula utriculi and the macula lagena (Sánchez-Calderón et al. 2007a; Sánchez-Guardado et al. 2013). In this developmental context, FGF3 and FGF16 could also contribute to the maculae specification. Experimental and descriptive evidence strongly supports this hypothesis. In *Fgf3* mutant mice (*int-2*^{neo}), the utricle and saccule do not show any indication of a separation into two parts (Mansour et al. 1993). In the commonest phenotype exhibited by affected *Fgf3* mutants, the utricle and saccule are fused with the enlarged cochlear duct (Hatch et al. 2007). In chick embryos, the *Fgf3* gene came to be expressed in the entire macula utriculi and in the rostral part of the macula sacculi (this work). Interestingly, an evident *Fgf16* expression delimited the presumptive territories of these maculae, entirely in the case of the macula utriculi and partially in that of the macula sacculi. The macula neglecta and macula lagena were included in areas with very weak *Fgf16* expressions. Therefore, two different molecular mechanisms mediated by FGF signaling pathways could regulate the specification of the anterior (utricular and saccular) and posterior (neglecta and lagena) maculae (see also Sánchez-Guardado et al. 2014).

Retinoic acid (RA) could regulate FGF activity in the developing otic epithelium. RA excesses and deficiencies lead to down-regulations of FGF3/FGF10 signaling molecules within the otic vesicle wall (Frenz et al. 2010; Cadot et al. 2012; see also Liu et al. 2008 for epithelial-mesenchymal interactions). The presence of putative sites in the *Fgf3* and *Fgf10* genes for a possible control by RA is consistent with those reports (Ohuchi et al. 2005). In the chick, the expression of *Raldh3* is firstly detected in the dorsomedial wall of the otocyst, in an area corresponding to the endolymphatic apparatus primordium (Sánchez-Guardado et al. 2009). Its expression extends ventrally to border the presumptive domain of sensory patches, defined at stage HH24 by the *Fgf10* expression (Sánchez-Guardado et al. 2013). Thus, RA could determine the specification of several sensory elements by the repression of *Fgf10* expression and the consequent subdivision of the early sensory *Fgf10*-expressing domain. Therefore, the spatial and temporal relationship of the *Fgf3*, *Fgf16*, and *Fgf10* expression patterns described in this work, together with other members of FGF family and RA, undoubtedly suggest their implication in an intricate molecular network leading to the maculae specification in the developing membranous labyrinth.

Specification of the auditory system

The basilar papilla, the organ of Corti in mammals, mediates hearing functions, which has no known counterpart in anamniote vertebrates (Fritzsch et al. 2013). Once the otic vesicle is formed, the auditory system develops in the emergent cochlear duct, a ventrally growing expansion in the ventralmost aspect of the otic anlagen. Chick *Fgf3* expression is detected in the ventral part, but not in the dorsal part, of the developing hindbrain, just in areas between contiguous rhombomeres (this work; Fig 1a; Aragón et al. 2005). Hence, an FGF3 hindbrain-derived signal could regulate the specification of the adjacent portion of the otic anlagen, the incipient cochlear duct (Hatch et al. 2007). SHH from the notochord and the

developing hindbrain floor plate is also necessary for the correct ventral patterning of the chick and mouse inner ears (Riccomagno et al. 2002, 2005; Bok et al. 2005, 2007). Therefore, FGF3 and SHH could cooperate to confer ventral otic identity onto the developing otic anlagen.

Fgf3 expression in the otic epithelium itself could also govern the specification of the ventral aspect of the otocyst in all vertebrate embryos (see the first part of this Discussion). Although ventrally expressed otic genes are not affected in the otic vesicle of several *Fgf3* mutants (Hatch et al. 2007), the cochlear duct appears to be enlarged and incorrectly coiled (Mansour et al. 1993), as well as severely misshapen or absent (Hatch et al. 2007). However, morphological studies of $Fgf3^{-/-}/Fgf10^{-/-}$ mutant embryos show smaller or normal cochlear ducts (Zelarayan et al. 2007). These findings strongly suggest that FGF3 from both the hindbrain and the otic epithelium itself migt be necessary, but not sufficient, for the specification of the ventral aspect of the otic anlagen. Other factors have to be involved in this developmental event. Those *Fgf3*-mutant morphological phenotypes are similar to that reported in *kreisler* mice (Deol 1964). Mouse *Six1* expression in the ventral otic vesicle is necessary for the activation of *Fgf3* and the maintenance of *Fgf10* and *Bmp4* expressions (Zheng et al. 2003). In this sense, the inner ear phenotype of *Six1*-mutant mice is comparable to that of *Shh*-mutant mice, with a loss or restriction of ventral molecular marker and a lack of the cochlear duct (Riccomagno et al. 2002; Ozaki et al. 2004).

Fgf3 expression has been reported in the developing auditory system at the later developmental stages (Wilkinson et al. 1989; Pickles 2001). Mutations in *Fgf3* are associated with syndromic deafness (Gregory-Evans et al. 2007; Tekin et al. 2007, 2008; Alsmadi et al. 2009; Riazuddin et al. 2011). Consequently, FGF3 could also be involved in cell fate specification. In chick embryos, a dorsoventral band of *Fgf3* expression was observed in the border of the developing *Fgf10*-positive basilar papilla at stages HH24–34 (this work). Concerning the *Fgf16* gene, its expression was observed in the caudal aspect of the otic anlagen at stage HH24, partially overlapping the *Fgf3* expression. Although this chick *Fgf16* expression disappears at later developmental stages (HH34; this work), mouse *Fgf16* expression has been detected in a small portion of the lateral margin of the cochlear duct, in which precursors of spiral prominence epithelial cells develop (Hatch et al. 2009). Therefore, FGF3 and FGF16 might cooperate in the early specification of the basilar papilla/organ of Corti and later cell differentiation in the hearing apparatus.

Specification of the cristae and semicircular canals

The cristae, and their associated semicircular canals, contribute to the codification of angular movements in all three cardinal planes. FGF3 could be directly involved in the induction and later specification of these components of the vestibular system. In zebrafish embryos, Mo-*fgf3* injections cause lack of semicircular canal protrusions (Léger and Brand 2002). In the mammalian inner ear, *Fgf3* (*int-2*) expression has been reported to be expressed in all sensory patches, including the crista in the ampulla of each semicircular canal (Wilkinson et al. 1989; see also Pirvola et al. 2000). In $int\text{-}2^{neo}$ mutants, the posterior semicircular canal is very much reduced at E13.5, the other canals being dilated at E15.5 (Mansour et al. 1993). Meticulous study of inner ear morphogenesis in *Fgf3* mutant mice with different grades of

genetic penetrance showed that, in addition to the endolymphatic apparatus anomalies, the anterior and posterior semicircular canals are absent or severally truncated, the associated ampullae being less affected (Hatch et al. 2007; see also Mansour et al. 1993). In addition, FGF3 and FGF10 might cooperate in the morphogenesis and differentiation of the semicircular canals: (1) *Fgf10* knockout mice show a loss of the posterior crista and the posterior canal, as well as a deformation of the anterior and lateral cristae and smaller anterior and lateral canals (Pauley et al. 2003); (2) local production of both FGF3 and FGF10 might act on the contiguous FGFR2(IIIb)-positive nonsensory epithelia as paracrine regulators of morphogenesis (Pirvola et al. 2000); and (3) only a single rudimentary canal is developed in $Fgf3^{-/-}/Fgf10^{-/-}$ and $Fgf3^{-/-}/Fgf10^{/+}$ mutant embryos (Zelarayan et al. 2007). In chick embryos, *Fgf3* and *Fgf19* expressions were observed in the borders of all cristae during development (this work and Sánchez-Calderón et al. 2007). Thus, chick FGF3/10/19 from the presumptive domains of the cristae could induce canal development, presumably by promoting *Bmp2* expression in the adjacent primordial canal pouches (Chang et al. 2004).

FGF16 could also be implicated in the specification of the semicircular system. In the chick inner ear, an evident *Fgf16* expression was detected early in a portion of the developing vertical and horizontal pouches (stages HH20, HH24, and HH27) and then in the proximal segment of their derivative semicircular canals (stage HH34). In the chick, the confrontation of the *Fgf10*-positive presumptive domains of all cristae, also expressing the *Fgf3* gene (see above), and the strongly *Fgf16*-expressing contiguous areas strongly suggests a direct involvement of these three genes in the specification of these sensory areas *versus* their associated non-sensory elements (this work). Interestingly, *Fgf16* could contribute to the outgrowth of semicircular primordial acting downstream of *Fgf10*, as it does in pectoral fin bud development by controlling cell proliferation in the mesenchyme and differentiation in the apical ectodermal ridge (Nomura et al. 2006). Interestingly, low levels of *Fgf16* expression were observed in the developing cristae at HH20–24. Mouse *Fgf16* expression is also present in all three cristae and in a portion of all adjacent semicircular canals (Hatch et al. 2009). Surprisingly, *Fgf16*-deficient inner ears are structurally and functionally normal (Hatch et al. 2009), suggesting a redundant role of FGF16 with other members of the FGF family.

It has recently been reported that the lateral crista could be originated by *de novo* creation in a territory expressing the *Serrate1* gene, just contiguous to the incipient *Fgf10*-positive macula utriculi (Sánchez-Guardado et al. 2013). The strong *Fgf19* expression observed in the clear-cut lateral border of the developing macula utriculi (Sánchez-Calderón et al. 2007a), abutting the *Fgf10*-negative lateral crista (Sánchez-Guardado et al. 2013), strongly suggested a possible cooperation of FGF family members in the specification of the two sensory patches, the lateral crista and the macula utricle, probably by setting up diffusion gradients that regulate positional identities of contiguous domains (Sánchez-Guardado et al. 2013). The juxtaposition of the *Fgf16*-positive lateral crista and the *Fgf3*-positive macula utriculi, located side by side, just prior to the specification of the first *Cath1*-positive hair cells in the lateral crista (stage HH24; this work), strongly supports this hypothesis. The heterogeneous *Fgf16* expression pattern observed at this level at stage HH27 (see short arrow in Fig 3e) fits well with this assumption. Since the horizontal canal and the lateral crista are considered new acquisitions in jawed vertebrates, the present finding could also be

considered in an evolutionary scenario (Sánchez-Guardado et al. 2013; reviewed by Fritzsch et al. 2006).

Hair cell specification

FGF3 could be openly involved in hair/supporting cell commitment. Concerning the otic epithelium itself, mouse *Fgf3* expression is present in developing sensory patches (Wilkinson et al. 1989; Pirvola et al. 2000). In the chick inner ear, *Fgf3* expression has also been observed in most of the sensory patches, except in the developing macula neglecta (this work). In the zebrafish otocyst, *Fgf3* and *Fgf8* are required for *Atoh1* expression (Millimaki et al. 2007), with *Fgf3*/*Fgf8* strongly enhancing the capability to act in response to *Atoh1* in the entire otic vesicle (Sweet et al. 2011). Also, mis-expression of zebrafish *Fgf3* in the rX of the hindbrain (rh5 plus rh6) is linked to the ectopic production of hair cells in the adjacent otic anlagen (Kwak et al. 2002). A direct involvement of FGF3 and FGF10 in mechano-sensory organ specification has also been indicated (Pirvola et al. 2000; see discussion in Nechiporuk and Raible 2008). However, *int-2*^{neo} mutants show a correct sensory differentiation in both vestibular and cochlear portions of the inner ear (Mansour et al. 1993), suggesting the implication of other factors in this developmental event. Regarding the *Fgf16* gene, very low levels of chick *Fgf16* expression were detected in a short period of cristae development (stage HH20 and HH24) and in a longer period for the macula neglecta and macula lagena (from stage HH24 onwards) (this work). Therefore, more studies are necessary to resolve the involvement of FGF3 and FGF16 in hair-cell specification. In this sense, SOX7 is a potential activator of FGF3 (Murakami et al. 2004), whereas SOX6 is a negative regulator (Murakami et al. 2001). The relationship between FGF3 and GATA family members in the patterning of the otic anlagen should be considered in future descriptive and experimental studies (Sinkkonen et al. 2011).

The formation of the acoustic-vestibular ganglion

Fgf3 is expressed in the neurogenic region of the otocyst and in the developing acoustic-vestibular ganglion (AVG) at least in mouse and chick embryos (McKay et al. 1996; Pirvola et al. 2000; Powles et al. 2004; Lillevali et al. 2006; Hatch et al. 2007; Frenz et al. 2010; this work). *Fgf3* mutant mice show a significant reduction of the VIIIth ganglion, which is displaced dorsomedially (*int-2*^{neo}: Mansour et al. 1993; *Fgf3*^{neo} mutants: Hatch et al. 2007). Since some *Fgf3*$^{-/-}$ mutant mice do not display any defects in neuroblast specification from the otic epithelium (Vázquez-Echeverría et al. 2008), FGF3 from the otic epithelium itself, as well as from the developing hindbrain, seems to be insufficient to govern otic neurogenesis. *Fgf3* and *Fgf10* are co-expressed in the neurogenic region of the otocyst (Pirvola et al. 2000; Wright and Mansour 2003; Hatch et al. 2007; Sánchez-Guardado et al. 2013; this work). Compensation between FGF3 and FGF10 should therefore be considered (Pirvola et al. 2000; see also Alvarez et al. 2003; Alsina et al. 2004; Vázquez-Echeverría et al. 2008). However, morphological studies of *Fgf3*$^{-/-}$/*Fgf10*$^{-/-}$ mutant embryos have shown an apparently normal acoustic-vestibular ganglion (Zelarayan et al. 2007). The participation of other FGF signaling pathways in AVG formation need to be tested (*Fgf8*, Sánchez-Calderón et al. 2004; *Fgf19*, Sánchez-Calderón et al. 2007b; *Fgf16*, this work for the acoustic ganglion).

Many transcription factors might participate in otic neurogenesis. *Fgf3* and *Lfng* are co-expressed rostroventrally in the mouse otic vesicle (Morli et al. 1998; Riccomagno et al. 2002; Ozaki et al. 2004; Raft et al. 2004; Hatch et al. 2007). *Six1*, together with *Eya1*, might control the initial selection of neuroblast precursors by the regulation of *Fgf3* expression, as well as other neurogenic markers, such as *Ngn1* and *Neurod1* (Zheng et al. 2003). Thus, *Fgf3* was absent in the *Six1*-deficient otic vesicle (Ozaki et al. 2004). In *Tbx1* null mutants, the expression domain of *Fgf3* loses its normal anterior restriction in the otocyst and expands into more posterior regions (Raft et al. 2004; Arnold et al. 2006). Besides, a medial expansion of *Fgf3* expression in the otocyst is clearly observed in *dreher* mutant mice, as well as the corresponding alteration of otic neurogenesis through an increased number of vestibular neuroblasts (Koo et al. 2009). Therefore, further studies are necessary to better comprehend the involvement of FGF and transcription factors in the formation of the acoustic-vestibular ganglion.

Acknowledgments

Grant sponsor: BFU2010-19461 (M.H.S.); BFU2005-09378-C02-01, BFU2008-04156, and SENECA 04548/GERM/06-10891 (L.P.). L-O.S-G. received a Junta-de-Extremadura predoctoral fellowship (PRE/08031).

We thank the members of our scientific group for helpful discussions. This work was supported by grants BFU2010-19461 and GR10152 (*Gobierno de Extremadura*) to Matías Hidalgo-Sánchez, and BFU2005-09378-C02-01 and BFU2008-04156 to Luis Puelles. L-O.S-G received a Junta-de-Extremadura predoctoral fellowship (PRE/08031).

ABBREVIATIONS

ac	anterior crista
AG	acoustic ganglion
asc	anterior semicircular canal
AVG	acoustic-vestibular ganglion
bp	basilar papilla
cc	common crus
cd	cochlear duct
ed	endolymphatic duct
es	endolymphatic sac
HB	hindbrain
hp	horizontal pouch
lc	lateral crista
lsc	lateral semicircular canal
ml	macula lagena

mn	macula neglecta
ms	macula sacculi
mu	macula utriculi
pc	posterior crista
psc	posterior semicircular canal
rh	rhombomere
s	saccule
tv	tegmentum vasculosum
u	utricle
vp	vertical pouch

References

Abello G, Khatri S, Radosevic M, Scotting PJ, Giraldez F, Alsina B. Independent regulation of Sox3 and Lmx1b by FGF and BMP signaling influences the neurogenic and non-neurogenic domains in the chick otic placode. Dev Biol. 2010; 339:166–178. [PubMed: 20043898]

Adam J, Myat A, Le Roux I, Eddison M, Henrique D, Ish-Horowicz D, Lewis J. Cell fate choices and the expression of Notch, Delta and Serrate homologues in the chick inner ear: parallels with Drosophila sense-organ development. Development. 1998; 125:4645–4654. [PubMed: 9806914]

Alsina B, Abello G, Ulloa E, Henrique D, Pujades C, Giraldez F. FGF signaling is required for determination of otic neuroblasts in the chick embryo. Dev Biol. 2004; 267:119–134. [PubMed: 14975721]

Alsmadi O, Meyer BF, Alkuraya F, Wakil S, Alkayal F, Al-Saud H, Ramzan K, Al-Sayed M. Syndromic congenital sensorineural deafness, microtia and microdontia resulting from a novel homoallelic mutation in fibroblast growth factor 3 (FGF3). Eur J Hum Genet. 2009; 17:14–21. [PubMed: 18701883]

Alvarez Y, Alonso MT, Vendrell V, Zelarayan LC, Chamero P, Theil T, Bosl MR, Kato S, Maconochie M, Riethmacher D, Schimmang T. Requirements for FGF3 and FGF10 during inner ear formation. Development. 2003; 130:6329–6338. [PubMed: 14623822]

Aragon F, Pujades C. FGF signaling controls caudal hindbrain specification through Ras-ERK1/2 pathway. BMC Dev Biol. 2009; 9:61. [PubMed: 19958530]

Aragon F, Vazquez-Echeverria C, Ulloa E, Reber M, Cereghini S, Alsina B, Giraldez F, Pujades C. vHnf1 regulates specification of caudal rhombomere identity in the chick hindbrain. Dev Dyn. 2005; 234:567–576. [PubMed: 16110512]

Arnold JS, Braunstein EM, Ohyama T, Groves AK, Adams JC, Brown MC, Morrow BE. Tissue-specific roles of Tbx1 in the development of the outer, middle and inner ear, defective in 22q11DS patients. Hum Mol Genet. 2006; 15:1629–1639. [PubMed: 16600992]

Battisti AC, Fekete DM. Slits and Robos in the developing chicken inner ear. Dev Dyn. 2008; 237:476–484. [PubMed: 18213576]

Bok J, Bronner-Fraser M, Wu DK. Role of the hindbrain in dorsoventral but not anteroposterior axial specification of the inner ear. Development. 2005; 132:2115–2124. [PubMed: 15788455]

Bok J, Chang W, Wu DK. Patterning and morphogenesis of the vertebrate inner ear. Int J Dev Biol. 2007; 51:521–533. [PubMed: 17891714]

Brigande JV, Kiernan AE, Gao X, Iten LE, Fekete DM. Molecular genetics of pattern formation in the inner ear: do compartment boundaries play a role? Proc Natl Acad Sci U S A. 2000; 97:11700–11706. [PubMed: 11050198]

Chang W, Brigande JV, Fekete DM, Wu DK. The development of semicircular canals in the inner ear: role of FGFs in sensory cristae. Development. 2004; 131:4201–4211. [PubMed: 15280215]

Chapman SC, Cai Q, Bleyl SB, Schoenwolf GC. Restricted expression of Fgf16 within the developing chick inner ear. Dev Dyn. 2006; 235:2276–2281. [PubMed: 16786592]

Chatterjee S, Kraus P, Lufkin T. A symphony of inner ear developmental control genes. BMC Genet. 2010; 11:68. [PubMed: 20637105]

Chen J, Streit A. Induction of the inner ear: stepwise specification of otic fate from multipotent progenitors. Hear Res. 2013; 297:3–12. [PubMed: 23194992]

Choo D, Ward J, Reece A, Dou H, Lin Z, Greinwald J. Molecular mechanisms underlying inner ear patterning defects in kreisler mutants. Dev Biol. 2006; 289:308–317. [PubMed: 16325169]

Deol MS. The Abnormalities of the Inner Ear in Kreisler Mice. J Embryol Exp Morphol. 1964; 12:475–490. [PubMed: 14207033]

Dominguez-Frutos E, Vendrell V, Alvarez Y, Zelarayan LC, Lopez-Hernandez I, Ros M, Schimmang T. Tissue-specific requirements for FGF8 during early inner ear development. Mech Dev. 2009; 126:873–881. [PubMed: 19619645]

Fekete DM. Cell fate specification in the inner ear. Curr Opin Neurobiol. 1996; 6:533–541. [PubMed: 8794105]

Fekete DM, Wu DK. Revisiting cell fate specification in the inner ear. Curr Opin Neurobiol. 2002; 12:35–42. [PubMed: 11861162]

Frenz DA, Liu W, Cvekl A, Xie Q, Wassef L, Quadro L, Niederreither K, Maconochie M, Shanske A. Retinoid signaling in inner ear development: A “Goldilocks” phenomenon. Am J Med Genet A. 2010; 152A:2947–2961. [PubMed: 21108385]

Freter S, Muta Y, Mak SS, Rinkwitz S, Ladher RK. Progressive restriction of otic fate: the role of FGF and Wnt in resolving inner ear potential. Development. 2008; 135:3415–3424. [PubMed: 18799542]

Fritzsch B, Pan N, Jahan I, Duncan JS, Kopecky BJ, Elliott KL, Kersigo J, Yang T. Evolution and development of the tetrapod auditory system: an organ of Corti-centric perspective. Evol Dev. 2013; 15:63–79. [PubMed: 23331918]

Fritzsch B, Pauley S, Beisel KW. Cells, molecules and morphogenesis: the making of the vertebrate ear. Brain Res. 2006; 1091:151–171. [PubMed: 16643865]

Gregory-Evans CY, Moosajee M, Hodges MD, Mackay DS, Game L, Vargesson N, Bloch-Zupan A, Ruschendorf F, Santos-Pinto L, Wackens G, Gregory-Evans K. SNP genome scanning localizes oto-dental syndrome to chromosome 11q13 and microdeletions at this locus implicate FGF3 in dental and inner-ear disease and FADD in ocular coloboma. Hum Mol Genet. 2007; 16:2482–2493. [PubMed: 17656375]

Groves AK, Fekete DM. Shaping sound in space: the regulation of inner ear patterning. Development. 2012; 139:245–257. [PubMed: 22186725]

Hamburger V, Hamilton HL. A series of normal stages in the development of the chick embryo. J Morphol. 1951; 88:49–92. [PubMed: 24539719]

Hans S, Westerfield M. Changes in retinoic acid signaling alter otic patterning. Development. 2007; 134:2449–2458. [PubMed: 17522161]

Hatch EP, Noyes CA, Wang X, Wright TJ, Mansour SL. Fgf3 is required for dorsal patterning and morphogenesis of the inner ear epithelium. Development. 2007; 134:3615–3625. [PubMed: 17855431]

Hatch EP, Urness LD, Mansour SL. Fgf16(IRESCre) mice: a tool to inactivate genes expressed in inner ear cristae and spiral prominence epithelium. Dev Dyn. 2009; 238:358–366. [PubMed: 18773497]

Hidalgo-Sanchez M, Alvarado-Mallart R, Alvarez IS. Pax2, Otx2, Gbx2 and Fgf8 expression in early otic vesicle development. Mech Dev. 2000; 95:225–229. [PubMed: 10906468]

Hill J, Clarke JD, Vargesson N, Jowett T, Holder N. Exogenous retinoic acid causes specific alterations in the development of the midbrain and hindbrain of the zebrafish embryo including positional respecification of the Mauthner neuron. Mech Dev. 1995; 50:3–16. [PubMed: 7605750]

Imamura T. Physiological functions and underlying mechanisms of fibroblast growth factor (FGF) family members: recent findings and implications for their pharmacological application. Biol Pharm Bull. 2014; 37:1081–1089. [PubMed: 24988999]

Itoh N, Ornitz DM. Evolution of the Fgf and Fgfr gene families. Trends Genet. 2004; 20:563–569. [PubMed: 15475116]

Karabagli H, Karabagli P, Ladher RK, Schoenwolf GC. Comparison of the expression patterns of several fibroblast growth factors during chick gastrulation and neurulation. Anat Embryol. 2002; 205:365–370. [PubMed: 12382140]

Kil SH, Streit A, Brown ST, Agrawal N, Collazo A, Zile MH, Groves AK. Distinct roles for hindbrain and paraxial mesoderm in the induction and patterning of the inner ear revealed by a study of vitamin-A-deficient quail. Dev Biol. 2005; 285:252–271. [PubMed: 16039643]

Koo SK, Hill JK, Hwang CH, Lin ZS, Millen KJ, Wu DK. Lmx1a maintains proper neurogenic, sensory, and non-sensory domains in the mammalian inner ear. Dev Biol. 2009; 333:14–25. [PubMed: 19540218]

Kwak SJ, Phillips BT, Heck R, Riley BB. An expanded domain of fgf3 expression in the hindbrain of zebrafish valentino mutants results in mis-patterning of the otic vesicle. Development. 2002; 129:5279–5287. [PubMed: 12399318]

Ladher RK, O'Neill P, Begbie J. From shared lineage to distinct functions: the development of the inner ear and epibranchial placodes. Development. 2010; 137:1777–1785. [PubMed: 20460364]

Leger S, Brand M. Fgf8 and Fgf3 are required for zebrafish ear placode induction, maintenance and inner ear patterning. Mech Dev. 2002; 119:91–108. [PubMed: 12385757]

Lillevali K, Haugas M, Matilainen T, Pussinen C, Karis A, Salminen M. Gata3 is required for early morphogenesis and Fgf10 expression during otic development. Mech Dev. 2006; 123:415–429. [PubMed: 16806848]

Lin Z, Cantos R, Patente M, Wu DK. Gbx2 is required for the morphogenesis of the mouse inner ear: a downstream candidate of hindbrain signaling. Development. 2005; 132:2309–2318. [PubMed: 15829521]

Liu W, Levi G, Shanske A, Frenz DA. Retinoic acid-induced inner ear teratogenesis caused by defective Fgf3/Fgf10-dependent Dlx5 signaling. Birth Defects Res B Dev Reprod Toxicol. 2008; 83:134–144. [PubMed: 18412219]

Lombardo A, Isaacs HV, Slack JM. Expression and functions of FGF-3 in Xenopus development. Int J Dev Biol. 1998; 42:1101–1107. [PubMed: 9879707]

Lufkin T, Dierich A, LeMeur M, Mark M, Chambon P. Disruption of the Hox-1.6 homeobox gene results in defects in a region corresponding to its rostral domain of expression. Cell. 1991; 66:1105–1119. [PubMed: 1680563]

Mahmood R, Kiefer P, Guthrie S, Dickson C, Mason I. Multiple roles for FGF-3 during cranial neural development in the chicken. Development. 1995; 121:1399–1410. [PubMed: 7789270]

Mahmood R, Mason IJ, Morriss-Kay GM. Expression of Fgf-3 in relation to hindbrain segmentation, otic pit position and pharyngeal arch morphology in normal and retinoic acid-exposed mouse embryos. Anat Embryol. 1996; 194:13–22. [PubMed: 8800419]

Mansour SL. Targeted disruption of int-2 (fgf-3) causes developmental defects in the tail and inner ear. Mol Reprod Dev. 1994; 39:62–67. [PubMed: 7999362]

Mansour SL, Goddard JM, Capecchi MR. Mice homozygous for a targeted disruption of the proto-oncogene int-2 have developmental defects in the tail and inner ear. Development. 1993; 117:13–28. [PubMed: 8223243]

Maroon H, Walshe J, Mahmood R, Kiefer P, Dickson C, Mason I. Fgf3 and Fgf8 are required together for formation of the otic placode and vesicle. Development. 2002; 129:2099–2108. [PubMed: 11959820]

Maves L, Jackman W, Kimmel CB. FGF3 and FGF8 mediate a rhombomere 4 signaling activity in the zebrafish hindbrain. Development. 2002; 129:3825–3837. [PubMed: 12135921]

McCarroll MN, Lewis ZR, Culbertson MD, Martin B, Kimelman D, Nechiporuk AV. Graded levels of Pax2a and Pax8 regulate cell differentiation during sensory placode formation. Development. 2012; 139:2740–2750. [PubMed: 22745314]

McKay IJ, Lewis J, Lumsden A. The role of FGF-3 in early inner ear development: an analysis in normal and kreisler mutant mice. Dev Biol. 1996; 174:370–378. [PubMed: 8631508]

Millimaki BB, Sweet EM, Dhason MS, Riley BB. Zebrafish atoh1 genes: classic proneural activity in the inner ear and regulation by Fgf and Notch. Development. 2007; 134:295–305. [PubMed: 17166920]

Morsli H, Choo D, Ryan A, Johnson R, Wu DK. Development of the mouse inner ear and origin of its sensory organs. J Neurosci. 1998; 18:3327–3335. [PubMed: 9547240]

Murakami A, Ishida S, Thurlow J, Revest JM, Dickson C. SOX6 binds CtBP2 to repress transcription from the Fgf-3 promoter. Nucleic Acids Res. 2001; 29:3347–3355. [PubMed: 11504872]

Murakami A, Shen H, Ishida S, Dickson C. SOX7 and GATA-4 are competitive activators of Fgf-3 transcription. J Biol Chem. 2004; 279:28564–28573. [PubMed: 15082719]

Nechiporuk A, Raible DW. FGF-dependent mechanosensory organ patterning in zebrafish. Science. 2008; 320:1774–1777. [PubMed: 18583612]

Nomura R, Kamei E, Hotta Y, Konishi M, Miyake A, Itoh N. Fgf16 is essential for pectoral fin bud formation in zebrafish. Biochem Biophys Res Commun. 2006; 347:340–346. [PubMed: 16815307]

Noramly S, Grainger RM. Determination of the embryonic inner ear. J Neurobiol. 2002; 53:100–128. [PubMed: 12382270]

Oh SH, Johnson R, Wu DK. Differential expression of bone morphogenetic proteins in the developing vestibular and auditory sensory organs. J Neurosci. 1996; 16:6463–6475. [PubMed: 8815925]

Ohuchi H, Yasue A, Ono K, Sasaoka S, Tomonari S, Takagi A, Itakura M, Moriyama K, Noji S, Nohno T. Identification of cis-element regulating expression of the mouse Fgf10 gene during inner ear development. Dev Dyn. 2005; 233:177–187. [PubMed: 15765517]

Ohyama T, Groves AK, Martin K. The first steps towards hearing: mechanisms of otic placode induction. Int J Dev Biol. 2007; 51:463–472. [PubMed: 17891709]

Ozaki H, Nakamura K, Funahashi J, Ikeda K, Yamada G, Tokano H, Okamura HO, Kitamura K, Muto S, Kotaki H, Sudo K, Horai R, Iwakura Y, Kawakami K. Six1 controls patterning of the mouse otic vesicle. Development. 2004; 131:551–562. [PubMed: 14695375]

Pauley S, Wright TJ, Pirvola U, Ornitz D, Beisel K, Fritzsch B. Expression and function of FGF10 in mammalian inner ear development. Dev Dyn. 2003; 227:203–215. [PubMed: 12761848]

Paxton CN, Bleyl SB, Chapman SC, Schoenwolf GC. Identification of differentially expressed genes in early inner ear development. Gene Expr Patterns. 2010; 10:31–43. [PubMed: 19913109]

Perez SE, Rebelo S, Anderson DJ. Early specification of sensory neuron fate revealed by expression and function of neurogenins in the chick embryo. Development. 1999; 126:1715–1728. [PubMed: 10079233]

Phillips BT, Bolding K, Riley BB. Zebrafish fgf3 and fgf8 encode redundant functions required for otic placode induction. Dev Biol. 2001; 235:351–365. [PubMed: 11437442]

Pickles JO, Chir B. Roles of fibroblast growth factors in the inner ear. Audiol Neurootol. 2002; 7:36–39. [PubMed: 11914524]

Pirvola U, Spencer-Dene B, Xing-Qun L, Kettunen P, Thesleff I, Fritzsch B, Dickson C, Ylikoski J. FGF/FGFR-2(IIIb) signaling is essential for inner ear morphogenesis. J Neurosci. 2000; 20:6125–6134. [PubMed: 10934262]

Powles N, Marshall H, Economou A, Chiang C, Murakami A, Dickson C, Krumlauf R, Maconochie M. Regulatory analysis of the mouse Fgf3 gene: control of embryonic expression patterns and dependence upon sonic hedgehog (Shh) signalling. Dev Dyn. 2004; 230:44–56. [PubMed: 15108308]

Raft S, Nowotschin S, Liao J, Morrow BE. Suppression of neural fate and control of inner ear morphogenesis by Tbx1. Development. 2004; 131:1801–1812. [PubMed: 15084464]

Revest JM, DeMoerlooze L, Dickson C. Fibroblast growth factor 9 secretion is mediated by a non-cleaved amino-terminal signal sequence. J Biol Chem. 2000; 275:8083–8090. [PubMed: 10713129]

Riazuddin S, Ahmed ZM, Hegde RS, Khan SN, Nasir I, Shaukat U, Butman JA, Griffith AJ, Friedman TB, Choi BY. Variable expressivity of FGF3 mutations associated with deafness and LAMM syndrome. BMC Med Genet. 2011; 12:21. [PubMed: 21306635]

Riccomagno MM, Martinu L, Mulheisen M, Wu DK, Epstein DJ. Specification of the mammalian cochlea is dependent on Sonic hedgehog. Genes Dev. 2002; 16:2365–2378. [PubMed: 12231626]

Riccomagno MM, Takada S, Epstein DJ. Wnt-dependent regulation of inner ear morphogenesis is balanced by the opposing and supporting roles of Shh. Genes Dev. 2005; 19:1612–1623. [PubMed: 15961523]

Riley BB, Phillips BT. Ringing in the new ear: resolution of cell interactions in otic development. Dev Biol. 2003; 261:289–312. [PubMed: 14499642]

Sanchez-Calderon H, Francisco-Morcillo J, Martin-Partido G, Hidalgo-Sanchez M. Fgf19 expression patterns in the developing chick inner ear. Gene Expr Patterns. 2007; 7:30–38. [PubMed: 16798106]

Sanchez-Calderon H, Martin-Partido G, Hidalgo-Sanchez M. Differential expression of Otx2, Gbx2, Pax2, and Fgf8 in the developing vestibular and auditory sensory organs. Brain Res Bull. 2002; 57:321–332. [PubMed: 11922981]

Sanchez-Calderon H, Martin-Partido G, Hidalgo-Sanchez M. Otx2, Gbx2, and Fgf8 expression patterns in the chick developing inner ear and their possible roles in otic specification and early innervation. Gene Expr Patterns. 2004; 4:659–669. [PubMed: 15465488]

Sanchez-Calderon H, Martin-Partido G, Hidalgo-Sanchez M. Pax2 expression patterns in the developing chick inner ear. Gene Expr Patterns. 2005; 5:763–773. [PubMed: 15979948]

Sanchez-Calderon H, Milo M, Leon Y, Varela-Nieto I. A network of growth and transcription factors controls neuronal differentation and survival in the developing ear. Int J Dev Biol. 2007; 51:557–570. [PubMed: 17891717]

Sanchez-Guardado LO, Ferran JL, Mijares J, Puelles L, Rodriguez-Gallardo L, Hidalgo-Sanchez M. Raldh3 gene expression pattern in the developing chicken inner ear. J Comp Neurol. 2009; 514:49–65. [PubMed: 19260055]

Sanchez-Guardado LO, Ferran JL, Rodriguez-Gallardo L, Puelles L, Hidalgo-Sanchez M. Meis gene expression patterns in the developing chicken inner ear. J Comp Neurol. 2011; 519:125–147. [PubMed: 21120931]

Sanchez-Guardado LO, Puelles L, Hidalgo-Sanchez M. Fgf10 expression patterns in the developing chick inner ear. J Comp Neurol. 2013; 521:1136–1164. [PubMed: 22987750]

Sanchez-Guardado LO, Puelles L, Hidalgo-Sanchez M. Fate map of the chicken otic placode. Development. 2014; 141:2302–2312. [PubMed: 24821982]

Schimmang T. Expression and functions of FGF ligands during early otic development. Int J Dev Biol. 2007; 51:473–481. [PubMed: 17891710]

Sienknecht UJ, Fekete DM. Comprehensive Wnt-related gene expression during cochlear duct development in chicken. J Comp Neurol. 2008; 510:378–395. [PubMed: 18671253]

Sienknecht UJ, Fekete DM. Mapping of Wnt, frizzled, and Wnt inhibitor gene expression domains in the avian otic primordium. J Comp Neurol. 2009; 517:751–764. [PubMed: 19842206]

Sinkkonen ST, Starlinger V, Galaiya DJ, Laske RD, Myllykangas S, Oshima K, Heller S. Serial analysis of gene expression in the chicken otocyst. J Assoc Res Otolaryngol. 2011; 12:697–710. [PubMed: 21853378]

Stevens CB, Davies AL, Battista S, Lewis JH, Fekete DM. Forced activation of Wnt signaling alters morphogenesis and sensory organ identity in the chicken inner ear. Dev Biol. 2003; 261:149–164. [PubMed: 12941626]

Storey KG, Crossley JM, De Robertis EM, Norris WE, Stern CD. Neural induction and regionalisation in the chick embryo. Development. 1992; 114:729–741. [PubMed: 1618139]

Sweet EM, Vemaraju S, Riley BB. Sox2 and Fgf interact with Atoh1 to promote sensory competence throughout the zebrafish inner ear. Dev Biol. 2011; 358:113–121. [PubMed: 21801718]

Tekin M, Hismi BO, Fitoz S, Ozdag H, Cengiz FB, Sirmaci A, Aslan I, Inceoglu B, Yuksel-Konuk EB, Yilmaz ST, Yasun O, Akar N. Homozygous mutations in fibroblast growth factor 3 are associated with a new form of syndromic deafness characterized by inner ear agenesis, microtia, and microdontia. Am J Hum Genet. 2007; 80:338–344. [PubMed: 17236138]

Tekin M, Ozturkmen Akay H, Fitoz S, Birnbaum S, Cengiz FB, Sennaroglu L, Incesulu A, Yuksel Konuk EB, Hasanefendioglu Bayrak A, Senturk S, Cebeci I, Utine GE, Tunçbilek E, Nance WE, Duman D. Homozygous FGF3 mutations result in congenital deafness with inner ear agenesis, microtia, and microdontia. Clin Genet. 2008; 73:554–565. [PubMed: 18435799]

Theil T, Frain M, Gilardi-Hebenstreit P, Flenniken A, Charnay P, Wilkinson DG. Segmental expression of the EphA4 (Sek-1) receptor tyrosine kinase in the hindbrain is under direct transcriptional control of Krox-20. Development. 1998; 125:443–452. [PubMed: 9425139]

Torres M, Giraldez F. The development of the vertebrate inner ear. Mech Dev. 1998; 71:5–21. [PubMed: 9507049]

Urness LD, Paxton CN, Wang X, Schoenwolf GC, Mansour SL. FGF signaling regulates otic placode induction and refinement by controlling both ectodermal target genes and hindbrain Wnt8a. Dev Biol. 2010; 340:595–604. [PubMed: 20171206]

Vazquez-Echeverria C, Dominguez-Frutos E, Charnay P, Schimmang T, Pujades C. Analysis of mouse kreisler mutants reveals new roles of hindbrain-derived signals in the establishment of the otic neurogenic domain. Dev Biol. 2008; 322:167–178. [PubMed: 18703040]

Vendrell V, Carnicero E, Giraldez F, Alonso MT, Schimmang T. Induction of inner ear fate by FGF3. Development. 2000; 127:2011–2029. [PubMed: 10769226]

Vendrell V, Vazquez-Echeverria C, Lopez-Hernandez I, Alonso BD, Martinez S, Pujades C, Schimmang T. Roles of Wnt8a during formation and patterning of the mouse inner ear. Mech Dev. 2013; 130:160–168. [PubMed: 23041177]

Walshe J, Maroon H, McGonnell IM, Dickson C, Mason I. Establishment of hindbrain segmental identity requires signaling by FGF3 and FGF8. Curr Biol. 2002; 12:1117–1123. [PubMed: 12121619]

Walshe J, Mason I. Fgf signalling is required for formation of cartilage in the head. Dev Biol. 2003; 264:522–536. [PubMed: 14651935]

Whitfield TT, Hammond KL. Axial patterning in the developing vertebrate inner ear. Int J Dev Biol. 2007; 51:507–520. [PubMed: 17891713]

Wright TJ, Mansour SL. Fgf3 and Fgf10 are required for mouse otic placode induction. Development. 2003; 130:3379–3390. [PubMed: 12810586]

Wu DK, Oh SH. Sensory organ generation in the chick inner ear. J Neurosci. 1996; 16:6454–6462. [PubMed: 8815924]

Yamada T, Placzek M, Tanaka H, Dodd J, Jessell TM. Control of cell pattern in the developing nervous system: polarizing activity of the floor plate and notochord. Cell. 1991; 64:635–647. [PubMed: 1991324]

Zelarayan LC, Vendrell V, Alvarez Y, Dominguez-Frutos E, Theil T, Alonso MT, Maconochie M, Schimmang T. Differential requirements for FGF3, FGF8 and FGF10 during inner ear development. Dev Biol. 2007; 308:379–391. [PubMed: 17601531]

Zhang X, Ibrahimi OA, Olsen SK, Umemori H, Mohammadi M, Ornitz DM. Receptor specificity of the fibroblast growth factor family. The complete mammalian FGF family. J Biol Chem. 2006; 281:15694–15700. [PubMed: 16597617]

Zheng W, Huang L, Wei ZB, Silvius D, Tang B, Xu PX. The role of Six1 in mammalian auditory system development. Development. 2003; 130:3989–4000. [PubMed: 12874121]

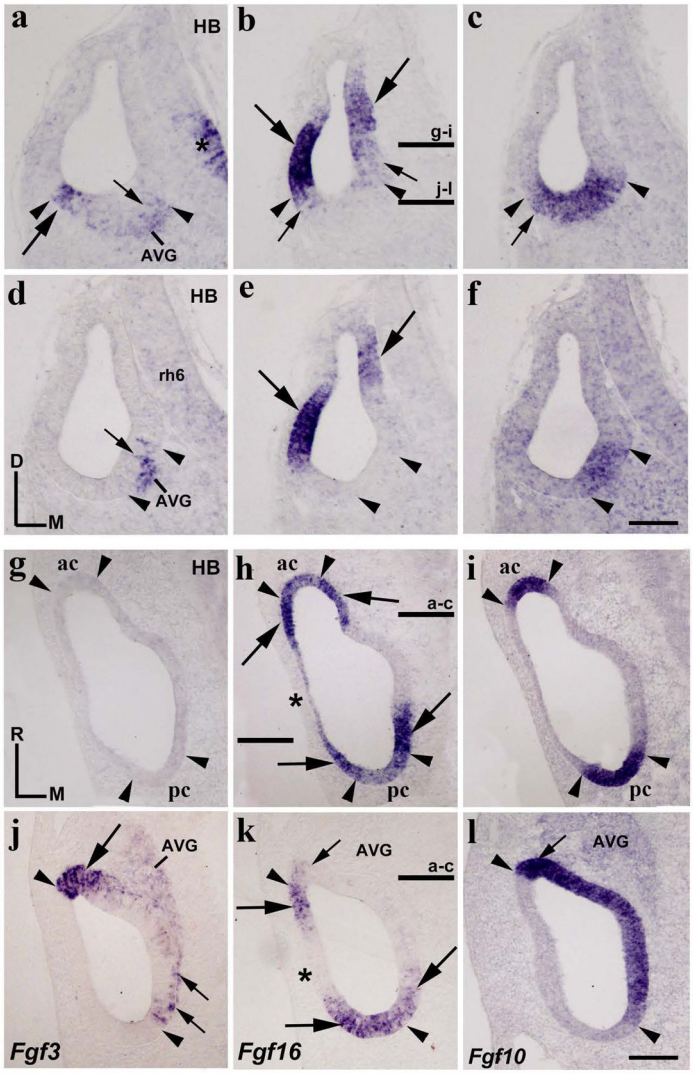

Figure 1. *Fgf3* and *Fgf16* expression patterns at the otic vesicle stage

Transverse (**a**–**f**) and horizontal (**g**–**l**) sections through the inner ear at stage HH20, indicated in **h**/**k** and **b**, respectively (see also Figs 5a and 5b for horizontal sections). The probes used are indicated in each column. The *Fgf10* expression defines the continuous anteroposterior sensory domain (between arrowheads in **c**, **f**, **i**, **l**). *Fgf3* expression was observed in the anteroventral portion of the otic anlagen (long arrows in **a**, **j**). Scattered cells with weak *Fgf3* expressions were also detected in the medial wall (short arrows in **a**, **d**, **j**). *Fgf3* expressions were always included within the *Fgf10*-positive sensory domain (see arrowheads in **a**, **c**, **d**, **f**, **j**, **l**). Heterogeneous *Fgf16* expression was detected at the anterior and posterior poles of the otic vesicle (long arrows in **b**, **e**, **h**, **k**), with the anterior and posterior cristae being included in them (ac and pc in **h**). The lateral wall was weakly labeled by the *Fgf16* expression dorsally (asterisk in **h**), but not ventrally (asterisk in **k**). No *Fgf16* expression was detectable in a portion of the medial wall (**h**, **k**). The stronger *Fgf3*-expressing anterior area (long arrows in **a**, **j**) showed weak *Fgf16* expression (short arrows in **b**, **k**). The arrowheads point to the boundaries of *Fgf10* expression, with some aspect of *Fgf3* and *Fgf16* expression

patterns being note. *Fgf3* expression was also observed in the developing acoustic-vestibular ganglion (AVG; **a**, **d**, **j**). In the neural tube, *Fgf3* expression was detected exclusively in the ventral part of interneuromeric areas (asterisk in **a**, **d**). For the abbreviations, see the list. Orientation: D, dorsal; M, medial; R, rostral. Scale bar = 8,3 μm in **f** (applies to **a**–**f**) and 12 μm in **l** (applies to **g**–**l**).

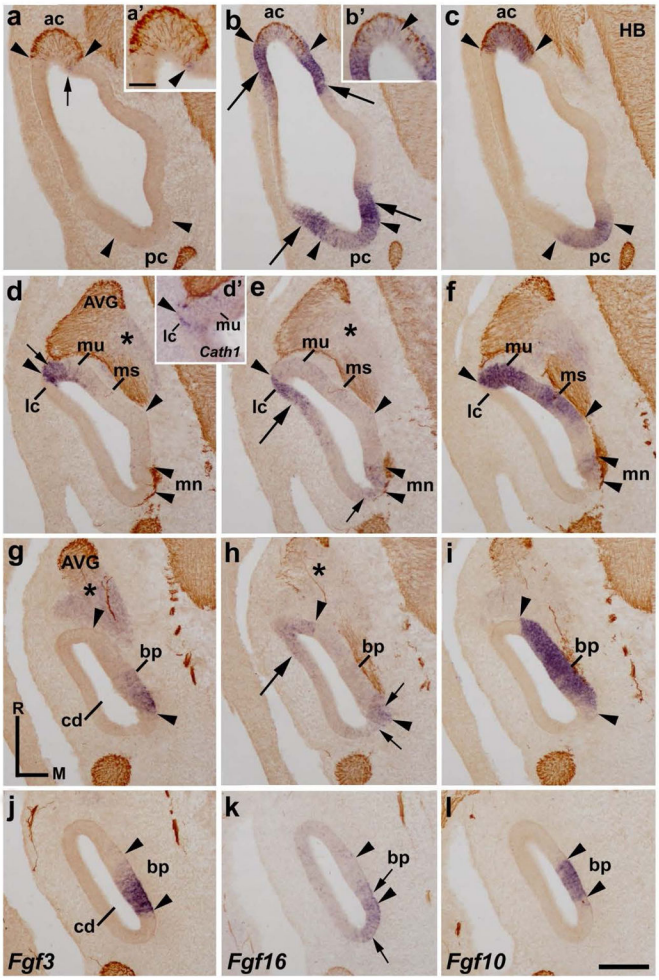

Figure 2. *Fgf3* and *Fgf16* expression patterns at HH24

Horizontal sections through the inner ear at stage HH24, indicated in Figs 5c and 5d. The probes used are indicated in each column. The sensory patches were *Fgf10* positive (between arrowheads in **c**, **f**, **i**, **l**). Sections were treated with 3A10 immunoreactions. The *Fgf3* transcripts were detected in the medial border of the anterior crista (ac; short arrows in **a**, **a′**), in the lateral portion of the macula utriculi (mu; short arrow in **d**), and in the caudal part of the basilar papilla (bp in **g**, **j**). An evident *Fgf16* expression bordered the anterior and posterior cristae (ac and pc; long arrows in **b**), both cristae displaying weak *Fgf16* expression (ac and pc in **b**; ac in **b′**). The *Fgf16* expression also bordered the lateral part of the macula utriculi (mu; long arrow in **e**) and the rostral part of the basilar papilla (long arrow in **h**). The *Fgf10*-negative and *Cath1*-positive lateral crista was labeled by *Fgf16* probes (lc in **d′**, **e**, **f**; also see the arrowheads at this level in **d**, **d′**, **e**, **f**). At the caudal pole of the otic anlagen, a weak *Fgf16*-expressing domain included the macula neglecta (mn; **e**) and a small portion of the basilar papilla (bp; **h**, **k**), in the latter overlapping partially with the *Fgf10*/*Fgf3*-expressing domain (bp; short arrows in **h**, **k**). The acoustic-vestibular ganglion (AVG) was *Fgf3* positive and *Fgf16* negative (asterisks in **d**, **e**, **g**, **h**). For the abbreviations, see the list. Orientation: M, medial; R, rostral. Scale bar = 25 μm in **a′** (applies to **a′**, **b′**, **d′**) and 31 μm in **m** (applies to **a**–**l**).

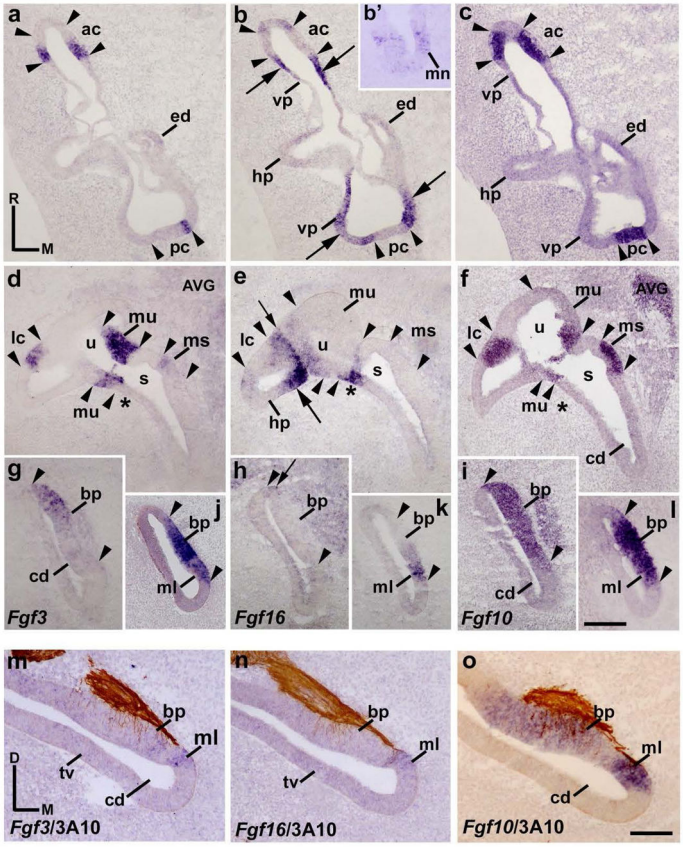

Figure 3. *Fgf3* and *Fgf16* expression patterns at HH27

a–**l**, Horizontal sections through the inner ear at stage HH27, indicated in Figs 5e and 5f. The probes used are indicated in each column. The *Fgf10* expression pattern defines the sensory patches (between arrowheads). The *Fgf3* transcripts were detected in borders of all cristae (ac, **a**; pc, **a**; lc, **d**). The entire macula utriculi and a part of the macula sacculi showed *Fgf3* expression (mu and ms in **d**). In the cochlear duct, the developing basilar papilla and the macula lagena showed *Fgf3* transcripts (bp and ml in **g**, **j**). Regarding the *Fgf16* gene, strong *Fgf16* expression was observed in the areas bordering all *Fgf10*-positive cristae (long arrows in **b**, **e**). The short arrow in **e** points to the border between the lateral semicircular system and the utricule. In the utricule (u) and saccule (s), parts of their walls were labeled by the *Fgf16* expression (u and asterisk in **e**). The macula neglecta and macula lagena were *Fgf16* positive (mn in **b**′; ml in **k**). The utricular and saccular maculae were *Fgf16* negative (mu and ms in **e**). The basilar papilla showed some *Fgf16*-staining cells (short arrow in **h**). **m**–**o**, transverse sections treated with 3A10 immunoreactions, showing the *Fgf3*/*Fgf16*-positive macula lagena and the portion of the basilar papilla. For the abbreviations, see the list. Orientation: M, medial; R, rostral. Scale bar = 27 μm in **l** (applies to **a**–**l**) and 20 μm in **o** (applies to **m**–**o**).

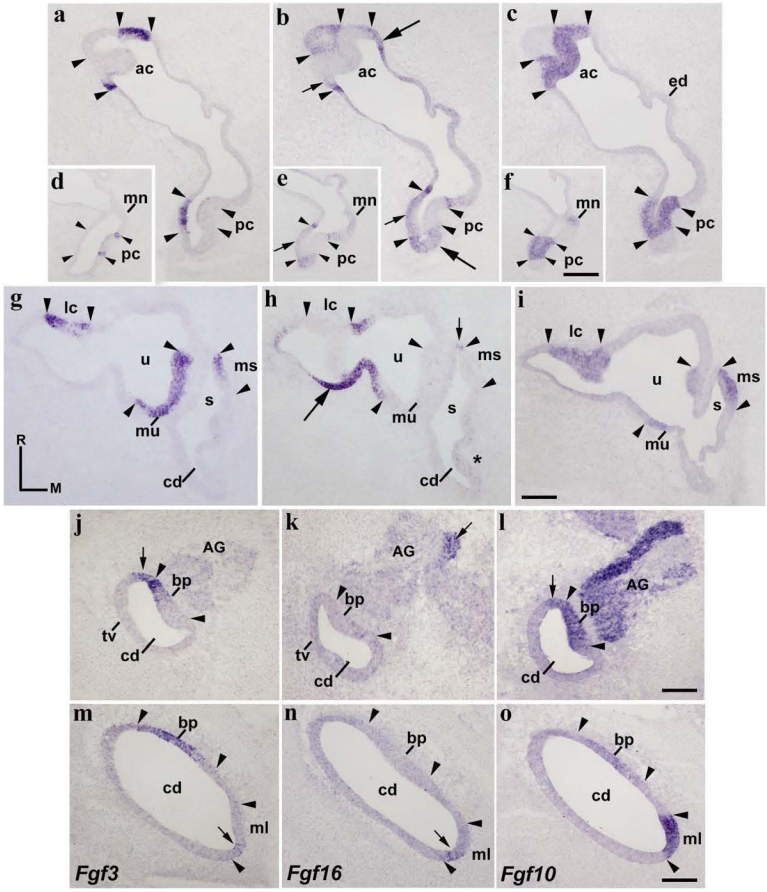

Figure 4. *Fgf3* expression pattern at HH34

Horizontal sections through the inner ear at stage HH34, indicated in Figs 5g and 5h. The probes used are indicated in each column. The borders of each *Fgf10*-positive sensory elements are indicated by arrowheads. *Fgf3* expression was detected in all cristae (ac, lc, and pc; **a**, **d**, **g**). The entire macula utriculi was *Fgf3* stained (mu in **g**). The rostral half of the macula sacculi showed a clear *Fgf3* expression (ms in **g**). In the cochlear duct, the rostralmost portion of the basilar papilla (bp in **j**, **l**, **m**, **o**) and the contiguous non-sensory epithelium (short arrows in **j**, **l**) were *Fgf3* positive. The macula lagena showed a few *Fgf3*-positive cells ventrally (short arrow in **m**). The *Fgf16* expression was observed in the non-sensory epithelium bordering all cristae (long arrows in **b**, **h**), as well as in part of the epithelium delimiting the utricular and saccular maculae (short arrows in **h** for the ms). A few *Fgf16*-expressing cells were observed in the border of the cristae (short arrows in **b**). The *Fgf3*-negative macula neglecta displayed a very weak *Fgf16* expression (mn in **d**, **e**). Most of the cochlear duct was devoid of *Fgf16* transcripts (cd; **k**, **n**), except for the macula lagena (ml in **n**). The acoustic ganglion showed a reduced group of *Fgf16*-expressing cells (AG; short arrow in **k**). For the abbreviations, see the list. Orientation: M, medial; R, rostral. Scale bar = 45 μm in **f** (applies to **d**–**f**), 33 μm in **i** (applies to **a**–**c**, **g**–**i**), 18 μm in **l** (applies to **j**–**l**), and 14 μm in **o** (applies to **m**–**o**).

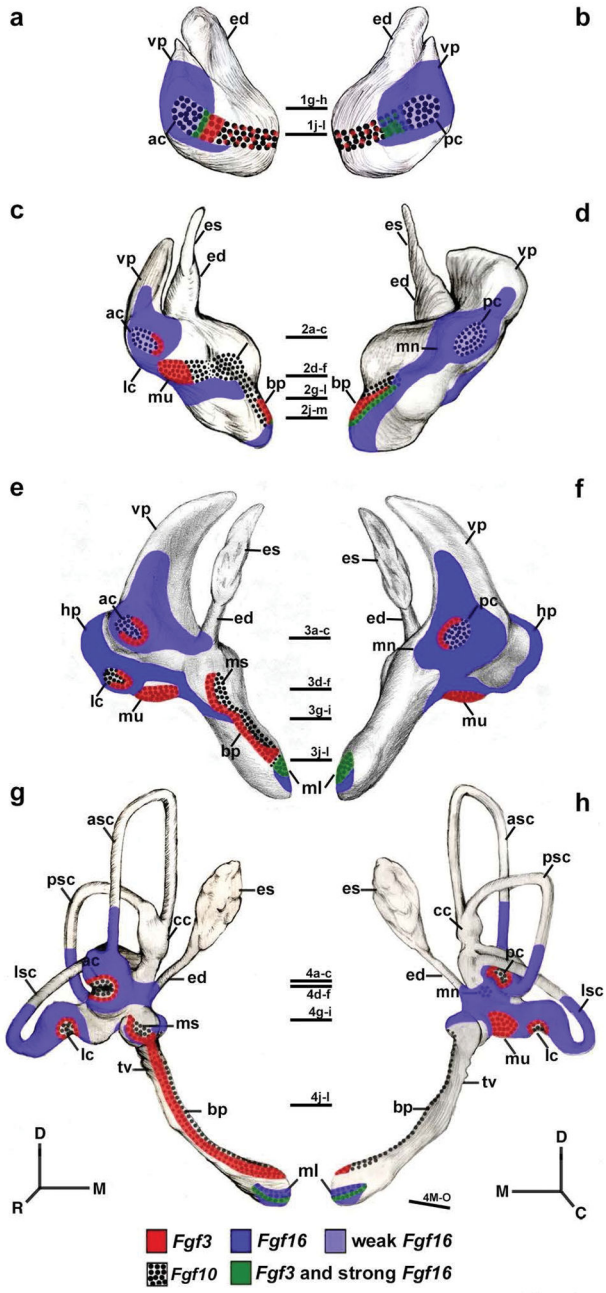

Figure 5.

Schematic drawings of the *Fgf3* and *Fgf16* expression patterns at stages HH20 (**a**, **b**), HH24 (**c**, **d**), HH27 (**e**, **f**), and HH34 (**g**, **h**). The horizontal sections illustrated in Figs 1, 2, 3, and 4 are indicated. Orientation: D, dorsal; M, medial; R, rostral; C, caudal.